CHEMISTRY
A EUROPEAN JOURNAL

FULL PAPER

DOI: 10.1002/chem.201201006

Discovering the Active Sites for C3 Separation in MIL-100(Fe) by Using Operando IR Spectroscopy

Stefan Wuttke,[a, b] Philippe Bazin,[a] Alexandre Vimont,[a] Christian Serre,[b] You-Kyong Seo,[c] Young Kyu Hwang,[c] Jong-San Chang,[c] Gérard Férey,[b] and Marco Daturi*[a]

Abstract: A reducible MIL-100(Fe) metal–organic framework (MOF) was investigated for the separation of a propane/propene mixture. An operando methodology was applied (for the first time in the case of a MOF) in order to shed light on the separation mechanism. Breakthrough curves were obtained as in traditional separation column experiments, but monitoring the material surface online, thus providing evidences on the adsorption sites. The qualitative and quantitative analyses of Fe^{II} and, to some extent, Fe^{III} sites were possible, upon different activation protocols. Moreover, it was possible to identify the nature and the role of the active sites in the separation process by selective poisoning of one family of sites: it was clearly evidenced that the unsaturated Fe^{II} sites are mainly responsible for the separation effect of the propane/propene mixture, thanks to their affinity for the unsaturated bonds, such as the C=C entities in propene. The activity of the highly concentrated Fe^{III} sites was also highlighted.

Keywords: active sites · hydrocarbon separation · IR spectroscopy · metal–organic frameworks · IR spectroscopy · reaction mechanisms

Introduction

Operando spectroscopy is a methodology that allows the investigation of a material during its working conditions. The Latin term operando derives from the field of heterogeneous catalysis, in which the spectroscopic characterisation of a catalytic material takes place during the reaction with the simultaneous measurement of catalytic activity/selectivity.[1,2] In contrast, in situ spectroscopy deals with the analysis of the material under controlled environments. The goal is a qualitative and quantitative characterisation of the surface species correlated with the catalytic performances of the material. Although the studied surface induces changes in comparison to the catalytic active one, an in situ study is always necessary before carrying out the operando experiments.[3] This is due to a better understanding of the surface species as well as the determination of their absorption coefficients under in situ conditions. Both techniques are complementary and necessary for the full understanding of the catalyst.[4,5] The simultaneous characterisation of the surface of the material as well as the functionality of a device under operation is also important in other fields (sensors, nanomaterials, energy, health etc.) of material science. Herein, we report for the first time, the infrared spectroscopic characterisation of a metal–organic framework (MOF) under flowing conditions for separation by using the operando methodology during the separation process.

MOFs are a new class of materials synthesised in a building-block fashion from metal-ion vertices. They are interconnected by organic linker molecules in a self-assembly process for the purpose of creating highly tailorable crystalline materials with pores of nanometre dimensions.[6] The infinite variations of the nature of the organic linkers added to the possibility of using di-, tri- (including rare earth) or tetravalent cations, lead to near-limitless possibilities for networks. One remarkable feature of MOFs is the virtual absence of dead volume, which principally gives them the highest porosities and record-holding surface areas.[7–9] In addition, the possibility of tuning the pore size, the presence of accessible coordinatively unsaturated metal sites (CUSs), functionalisations of the organic linkers (by using functionalised ligands during the synthesis[10] or post-synthetic modification (PSM) of the linker[11]) and the easy, inexpensive synthesis of MOFs make this new class of materials suitable for different applications for example, catalysis,[12–16] selective gas adsorption and separation,[17–19] gas storage[17,20,21] or drug deliv-

[a] Dr. S. Wuttke, Dr. P. Bazin, Dr. A. Vimont, Prof. M. Daturi
Laboratoire Catalyse et Spectrochimie
ENSICAEN, Université de Caen, CNRS, 6
Boulevard Maréchal Juin, 14050 Caen (France)
Fax: (+33) 31452822
E-mail: marco.daturi@ensicaen.fr

[b] Dr. S. Wuttke, Dr. C. Serre, Prof. G. Férey
Institut Lavoisier (UMR CNRS 8180)
Université de Versailles Saint-Quentin-en-Yvelines
45, Avenue des Etats-Unis, 78035 Versailles (France)

[c] Dr. Y.-K. Seo, Dr. Y. K. Hwang, Dr. J.-S. Chang
Biorefinery Research Group
Catalysis Center for Molecular Engineering
Korea Research Institute of Chemical Technology (KRICT)
Jang-dong 100, Yuseong, Daejeon 305-600 (South Korea)

ery.[22–25] From an industrial point of view, the application of MOFs for separation questions is probably the most promising field. One of the greatest expenses in chemical industry is in fact related to the separation and purification of the desired products. In the field of separation and purification distillation is the most common unit of operation; however, it becomes energetically unfavourable and unpractical when boiling points are close, or when the mixture contains compounds that are unstable or reactive at elevated temperatures. Unfortunately, the by-products are most of the time chemically and physically similar to the desired product. An interesting alternative is separation by preferential gas adsorption. The high surface area of MOFs as well as the different possible interactions of the compounds in these materials qualify them as good candidates for environmentally friendly gas adsorbents with preferential gas sorption properties.[26]

This report concerns the study of MIL-100(Fe) (MIL stands for Materials of Institut Lavoisier), the presence and amount of Fe^{II} and Fe^{III} CUS and their role for the separation of a propane/propene mixture through the use of the infrared operando methodology. Recently, some of us reported that MIL-100(Fe) can be used for the separation of propane/propene.[27] It was shown that by increasing the activation temperature of the sample, the separation effect increases; unfortunately, by increasing the partial pressure, the separation effect decreases. By using the operando approach, it has been possible to investigate the material at a molecular level and, therefore, to describe the iron site formation and action on the working surface versus the reaction parameters. Moreover, by selectively blocking one of the iron sites with a probe molecule, it has been shown its influence for the separation process. Through that, we have discriminated the active sites in MIL-100(Fe) that are responsible for the separation of the propane/propene mixture. Therefore, this work aims at providing an important contribution to a better understanding of MOF materials and their applications as well as to a widening of the field of operando characterisation to other domains than catalysis. In fact, there are just a few existing articles that study the redox properties of MOFs[28] and, to the best of our knowledge, this is the first study that investigates the redox properties of a MOF through operando IR spectroscopy.

Results and Discussion

C_3H_8/C_3H_6 separation with MIL-100(Fe): We start showing the behaviour of the investigated sample in contact with a propane/propene flow. Sending a propane/propene gas mixture in a He flow through the sample, followed by mass spectrometry ($m/z=29$ for C_3H_8 and $m/z=41$ for C_3H_6), revealed that both gases are adsorbed. While an activation temperature increase leads to a greater amount of propene adsorbed onto MIL-100(Fe) (Figure 1), on the contrary, a similar amount of propane was adsorbed at each temperature; therefore, just one example of the breakthrough curve

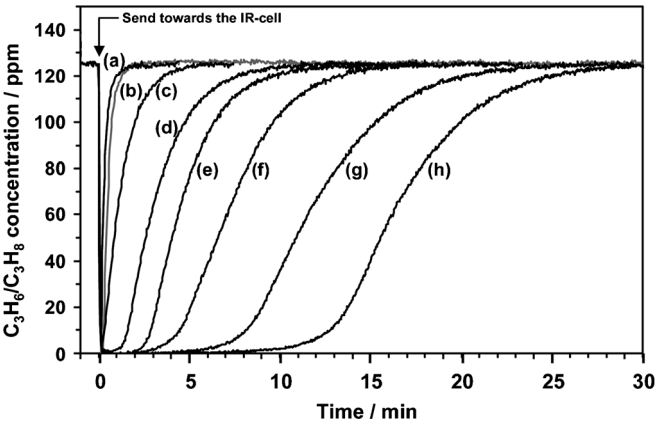

Figure 1. C_3H_6 (black)/C_3H_8 (grey) adsorption at 298 K on MIL-100(Fe) activated at different temperatures for 3 and 12 h followed by mass spectrometry ($m/z=29$ for C_3H_8 and $m/z=41$ for C_3H_6). a) Blank experiment without sample for both C_3H_6 and C_3H_8; b) C_3H_8 curves (similar curves whatever the pre-treatment (temperature and time); C_3H_6 curves for an activation at c) 373 K for both 3 and 12 h; d) 423 K for both 3 and 12 h; e) 473 K for 3 h; f) 473 K for 12 h; g) 523 K for 3 h; h) 523 K for 12 h.

for C_3H_8 is represented in Figure 1 (line b, grey colour). In parallel, IR spectra were recorded: they clearly showed the bands for adsorbed propene,[29,30] as illustrated in Figure 2A for MIL-100(Fe) activated at 523 K for 3 h. Indeed, a recent IR study led by Leclerc et al.[29] shows that adsorption of propane on MIL-100(Fe) gives rise to two IR bands at $\tilde{\nu}=$ 2868 and 2958 cm^{-1} assigned to the overtone $2\delta(CH_3)$ and the fundamental $\nu(CH_3)$ modes, respectively. By using propene, the infrared spectrum recorded clearly shows different characteristic bands in the $\tilde{\nu}=2800$–$3100\ cm^{-1}$ range. Among these bands, the $\nu_s(CH_3)$ mode at $\tilde{\nu}=2930\ cm^{-1}$ and the $\nu(C{=}C)+\delta_{as}(CH_3)$ combination at $\tilde{\nu}=3060$ or 3048 cm^{-1}, as the propene interacts with Fe^{III} or Fe^{II} sites, can be taken as indicative for the olefin adsorption. Thus, plotting the area for the propene $\nu_s(CH_3)$ band at $\tilde{\nu}=2930\ cm^{-1}$[29] versus time (Figure 2B) reveals the kinetics of olefin adsorption. Moreover, the comparison of the IR spectra at saturation for C_3H_6/C_3H_8 adsorption confirms the increase in the adsorption of propene (essentially on Fe^{II}) by increasing the activation temperature (Figure 2C). The correlation between the preferential propene adsorption and the sample activation temperature increase is demonstrated by the plot of the band area for $\nu_s(CH_3)$ versus the amount of disappeared C_3H_6 calculated from mass spectrometry results (Figure 2D). These results are coherent with calorimetric experiments: an initial adsorption heat of $-30\ kJ\,mol^{-1}$ was found for propane, whereas for propene the adsorption heat depends on the activation temperature ($\approx -50\ kJ\,mol^{-1}$ for MIL-100(Fe) activated at 423 K and $\approx -70\ kJ\,mol^{-1}$ for MIL-100(Fe) activated at 523 K).[27] An explanation for this behaviour of MIL-100(Fe) was attributed to the formation of increasing amounts of Fe^{II} sites. The presence of an additional d electron in the Fe^{II} orbitals causes in fact a π-backdonation interaction with the olefin molecules. Here, the electron density of the d orbitals of the Fe^{II} atoms is transferred to the π^* orbital of the unsaturated gas molecule

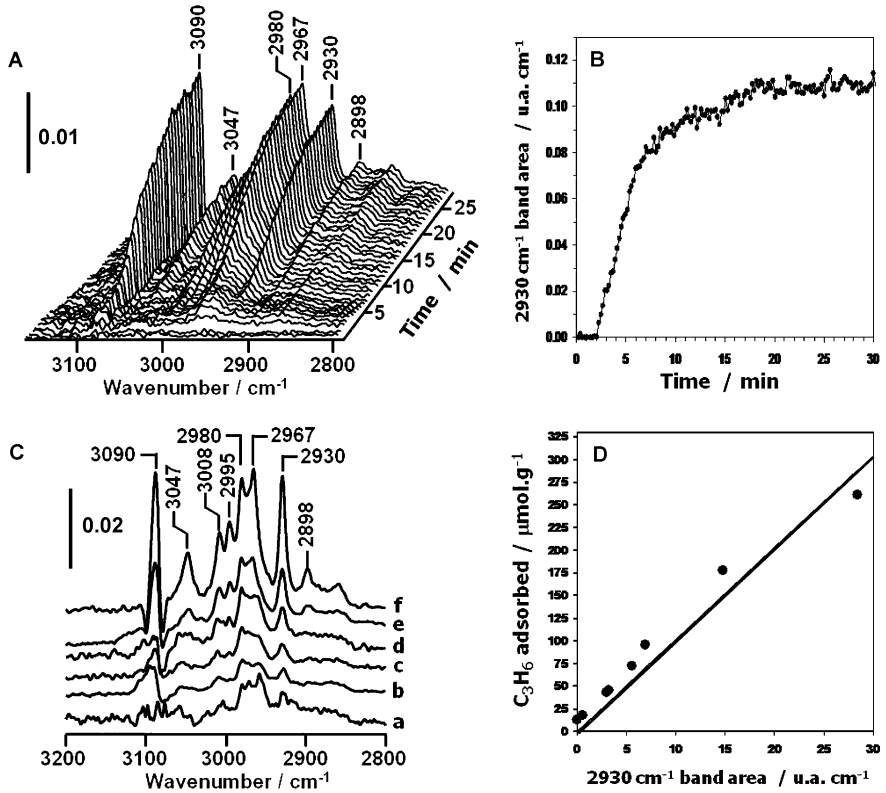

Figure 2. A) IR spectra versus time recorded during the C_3H_6/C_3H_8 adsorption at 298 K on MIL-100(Fe) activated at 523 K for 3 h. B) $\tilde{\nu}=2930\ cm^{-1}$ band area evolution. C) IR spectra at saturation for C_3H_6/C_3H_8 adsorption on MIL-100(Fe) activated at a) 373/3, b) 373/12, c) 473/3, d) 473/12, e) 523/3 and f) 523 K/12 h. D) $\tilde{\nu}=2930\ cm^{-1}$ band area at saturation versus the amount of C_3H_6 adsorbed evaluated by mass spectrometry ($m/z=41$) for each condition of pre-treatment.

(LUMO) and therefore, increases the stability of the metal–adsorbate complex. On the other hand, the Fe^{III} CUS act as pure Lewis acid sites (electron-pair acceptors) by interacting with the olefin. Thus, only a weak interaction is possible between propane and the CUSs of MIL-100(Fe), which leads to nearly no adsorption under the flow conditions used during the separation process. A first clue indicating the interaction of propene with the Fe^{II} sites is the presence of the band at $\tilde{\nu}=3047\ cm^{-1}$ (Figures 2A and C), assigned to a $\nu(C{=}C)+\delta_{as}(CH_3)$ combination mode, sensitive to the interaction with the CUSs, conversely giving rise to a band at around $\tilde{\nu}=3060\ cm^{-1}$ when the interaction takes place with Fe^{III} species.[29] The increase of the band at $\tilde{\nu}=3047\ cm^{-1}$ by increasing the activation temperature, as well as the absence of the band at $\tilde{\nu}=3060\ cm^{-1}$, supports the statements above (Figure 2C). However, for a full understanding of the gas separation phenomena, a characterisation of the sample under the separation flow conditions is necessary and is reported below.

Thermal behaviour: Having ascertained that the propene separation effect is connected with an increase of the Fe^{II} concentration, it is now necessary to understand how these sites are created. The thermal behaviour of MIL-100(Fe) was previously investigated by using a thermal analysis under an oxygen flow.[31] Thermogravimetric analysis (TGA) indicated three instances of weight loss between 298 and 873 K. The first, (40.1% in weight) at 373 K, was attributed to the departure of free water molecules inside the pores, followed by the second, a slow release of bound water between 373 and 473 K and, finally, the destruction of the framework at about 573 K. For the breakthrough test for the separation of propane/propene, MIL-100(Fe) was activated in a helium flow at different temperatures before being found active.[27] It is well known that water can be adsorbed on the CUSs,[32] hence the departure temperature of water is a very important phenomenon and can contribute to the separation effect of MIL-100(Fe). The IR spectra revealing the progressive departure of water are shown in Figure 3. Only the ν(OH) region is shown, because the intense bands due to carboxylate groups of the material framework below $\tilde{\nu}=1700\ cm^{-1}$ hide the $\delta(H_2O)$ mode.[10] The broad band between $\tilde{\nu}=3600$ and $3200\ cm^{-1}$ is typical for OH groups of adsorbed water ($\nu(H_2O)$), which undergo hydrogen bonding. On the other hand, the sharp bands in the $\tilde{\nu}=3600$–$3700\ cm^{-1}$ range are due to the presence of hydroxyl groups

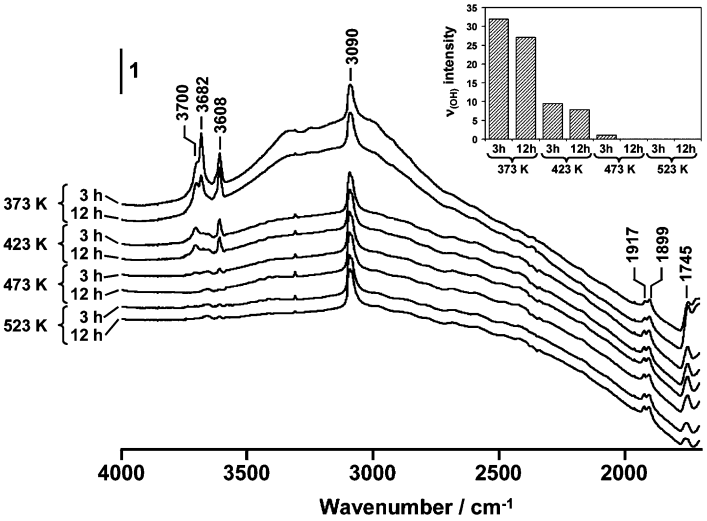

Figure 3. IR spectra of MIL-100(Fe) heated at different temperatures for 3 or 12 h under a helium flow.

of water coordinated to CUSs, showing a lack of OH groups in MIL-100(Fe) as it was the case for the isostructural MIL-100(Cr),[29,32,33] and as it was also confirmed recently in the dehydrated MIL-100(Fe), indeed.[29] These bands decrease at the same time as the broad $\nu(H_2O)$ band in the $\tilde{\nu}=3600$–$3200\ cm^{-1}$ region disappear at a relatively low temperature (≈ 373 K). The water bands further decrease in intensity after 423 K and finally disappear at 473 K (Figure 3). Therefore, these results indicate that the complete desorption of free and bound water molecules from MIL-100(Fe) occurs at 473 K under a helium flow. In turn, it reveals the strong presence of water below 373 K and residuals at 423 K. While heating the sample to 423 K, it is probable that the huge water departure is due to the desorption of free water molecules inside the pores, followed by the desorption of bounded water molecules at 473 K, in agreement with the TGA results.[31] It is worth noticing that the extent of the thermal treatment (3 or 12 h) has less influence on the presence of water (Figure 3), meaning that at a fixed temperature a pseudo-equilibrium state is reached. Additionally, the $\nu(CH_3)$ band at $\tilde{\nu}=3090\ cm^{-1}$ unchanged upon temperature treatment, is witnessing that the structure is completely stable until 523 K, again in agreement with the TGA results founding framework destruction at about 573 K.[31]

So, the thermal treatment provokes water desorption, at the same time that it increases the amount of adsorbed propene on Fe^{II}, as shown in the previous paragraph. Is there a direct correlation between these two phenomena? IR spectroscopy of adsorbed probe molecules can answer this question, as shown below.

Dynamic probe of Fe^{II}/Fe^{III} CUSs sending a flow of adapted molecules: The effect of the thermal activation of MIL-100(Fe) on the amount of Fe^{II} and Fe^{III} CUSs was studied through CO and NO adsorption at room temperature by using a gas flow. The use of CO as a suitable probe molecule has already been pointed out.[34] NO is a more reactive probe molecule, therefore it is used less often as an IR probe for the characterisation of the state of the metal ions.[35] Nevertheless, the combination of both CO and NO was already found as an optimum way to fully characterise iron oxidation and coordination states in porous compounds.[36]

Figure 4 shows the IR spectra of the CO and NO adsorption stretching region on MIL-100(Fe), activated at different temperatures for 3 and 12 h. CO adsorption gives rise to three $\nu(CO)$ bands at $\tilde{\nu}=2189$, 2182 and $2175\ cm^{-1}$. The band at $\tilde{\nu}=2189\ cm^{-1}$ appears weak in intensity by an activation temperature of 373 K for 3 h. It increases by an activation temperature of 423 K and finally the intensity does not change by increasing the activation temperature. This weak band can be assigned to the interaction of CO with Fe^{III} CUSs.[29,37] The blue shift ($\Delta(\tilde{\nu}=(CO))=2189\ cm^{-1}-2143\ cm^{-1}=45\ cm^{-1}$) of the $\nu(CO)$ mode indicates that a Fe^{III} CUS in MIL-100(Fe) is a weak Lewis acidic site. Therefore, the weakness of the interaction cannot allow a complete detection of these sites at the measuring conditions (room temperature and under flow with a weak partial pressure of CO). On the other hand, two other bands appear at $\tilde{\nu}=2182$ and $2175\ cm^{-1}$, being weak after activation at 423 K for 3 h, then increasing in intensity upon thermal treatment at higher temperatures. Both bands can be assigned to CO adsorbed on Fe^{II} CUSs.[29,38] The sample was submitted to different concentrations of CO (0.5–40%) in the He flow. By using a 10% CO stream, a plateau for the intensity of the bands at $\tilde{\nu}=2182$ and $2175\ cm^{-1}$ (corresponding to the saturation of the Fe^{II} CUSs by CO) was observed. Hence, 10% CO in a He flow was chosen as the most adapted gas mixture for the complete detection of Fe^{II} CUSs. Figure 5A shows the effect of the temperature and the time on the area of the peaks identifying Fe^{II} and Fe^{III} CUSs. The presence of Fe^{II} CUSs starts weakly after the treatment at 373 K and increases with time and temperature, particularly after activation between 473 and 523 K. In contrast, the presence of Fe^{III} CUSs increases with a treatment at 423 K and remains nearly unchanged at higher temperature. There is a perfect correlation between the amount of Fe^{III} CUSs probed by CO (Figure 5A) and the departure of water (Figure 3). The much stronger stability of the carbonyl species on Fe^{II} CUSs can be explained by the π-back-donation effect, which stabilises the CO molecule on Fe^{II} CUSs and causes a red shift of the $\nu(CO)$ mode, as already pointed out.[39]

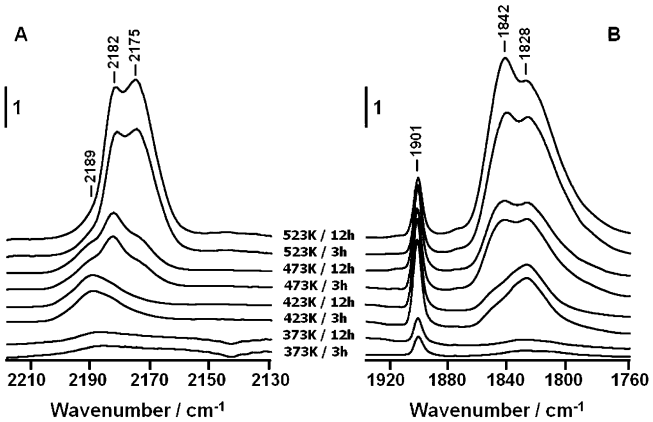

Figure 4. IR spectra of MIL-100(Fe) under A) CO (10% of CO in He, 25 cc min) or B) NO (1% NO in He, 25 cc min) flow at RT after activation of the sample under He flow at different temperatures for 3 or 12 h.

Figure 4B shows the IR spectra for NO adsorbed on MIL-100(Fe) activated at different temperatures for 3 and 12 h. In our conditions, NO_2, N_2O and N_2 are not detected, therefore we can consider NO as no reacting. Three $\nu(NO)$ bands are present at $\tilde{\nu}=1901$, 1842 and $1828\ cm^{-1}$. The band at $\tilde{\nu}=1901\ cm^{-1}$ can be assigned to nitrosyls on Fe^{III} CUSs and the doublet at $\tilde{\nu}=1842$ and $1828\ cm^{-1}$ to species coordinated on Fe^{II} CUSs.[40,41] The NO bands on the different iron sites show exactly the same behaviour as the corresponding bands for CO. A very small amount of Fe^{II} sites is observed at 373 K and the NO band for Fe^{III} sites does not increase in intensity above an activation temperature of 423 K. Again, a complete detection of all Fe^{III} CUSs is not possible by send-

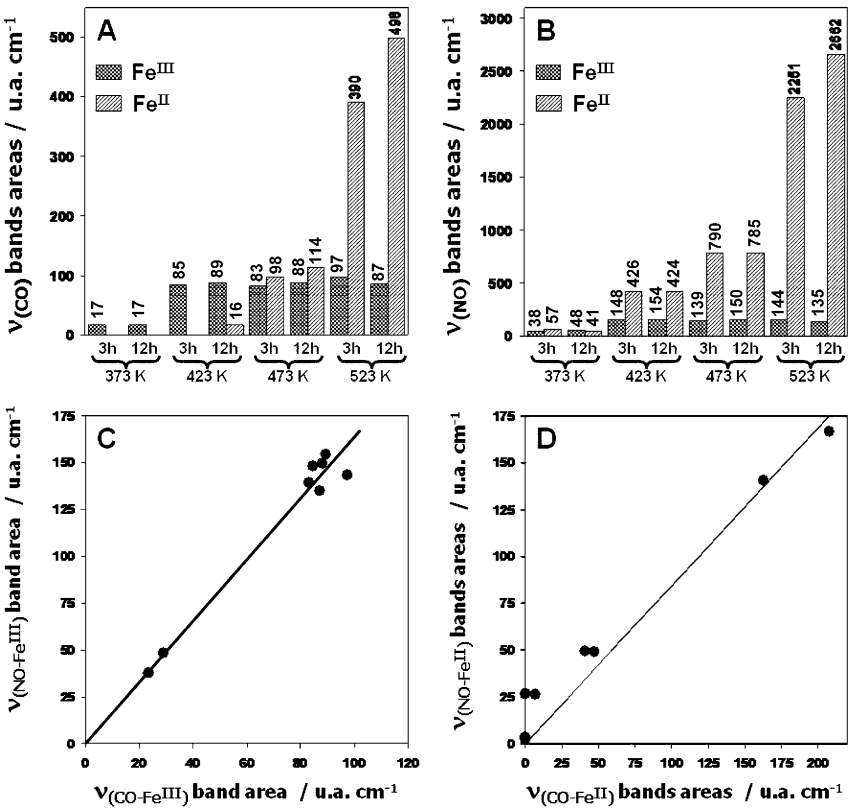

Figure 5. Development of the band area, which corresponds to Fe^{II} and Fe^{III} CUSs detected by A) CO and B) NO. Correlation between the band area for C) Fe^{III} and D) Fe^{II} detected by CO (*x* axis) and NO (*y* axis).

ing a NO flow (1% in He) at room temperature, due to the weak interaction between the molecule and the weak Lewis acidic sites. This weak interaction is confirmed by the departure of the band at $\tilde{\nu}=1901\ cm^{-1}$ assigned to nitrosyls on Fe^{III} CUSs, in the spectrum recorded after the elimination of NO in the flow (this point will be discussed in detail in the following part). Figures 5A and B display the effect of the treatment temperature and the time on the peak area of carbonyls and nitrosyls on Fe^{II} and Fe^{III} CUSs. The results presented in Figure 5B match very well with the CO adsorption results presented in Figure 5A. This is underlined by plotting the band area of Fe^{II} CUSs detected by CO versus the area of Fe^{II} CUSs detected by NO (Figure 5D); the same plot is obtained for Fe^{III} CUSs (Figure 5C). It is interesting to remark that a huge amount (about 250 $\mu mol\,g^{-1}$) of the Fe^{II} CUSs is produced by heating MIL-100(Fe) at 523 K. The investigations on water removal reported above have clearly indicated that nearly all water has evolved from the sample under flow at 473 K. Therefore, an increase of the site concentration is not (or not only) connected with the departure of water, but could rather be associated with the departure of anionic ligands (F^- and/or OH^-), which need a higher temperature to be desorbed.[27]

These results are extremely informative, nevertheless is worth of interest knowing if they have been affected in some way by the choice of the probe molecules, which allowed discriminating and numbering the adsorption sites. To be sure of our results, we have verified this point.

Have the probe molecules affected the Fe^{II}/Fe^{III} CUS ratio?—stability of the Fe^{II} and Fe^{III} CUSs: An important factor to be ascertained is whether the adsorbed probe molecules might have influenced the measured characteristics of the probed solid. In fact, one of the basic requirements for the use of a probe molecule is its inertia towards changes in the surface properties of the investigated material. Therefore, desorption and re-adsorption experiments were performed to verify the eventual responsibility of the probe molecules towards site creation on the surface of MIL-100(Fe), especially in the case of NO.

Changing the flow from 10% of CO in He (Figure 6a) to pure He results in a complete disappearance of all carbonyl bands (Figure 6b). Therefore, CO on Fe^{II} and Fe^{III} CUSs in MIL-100(Fe) is not stable under an inert flow at room temperature. Moreover, introducing again a gas

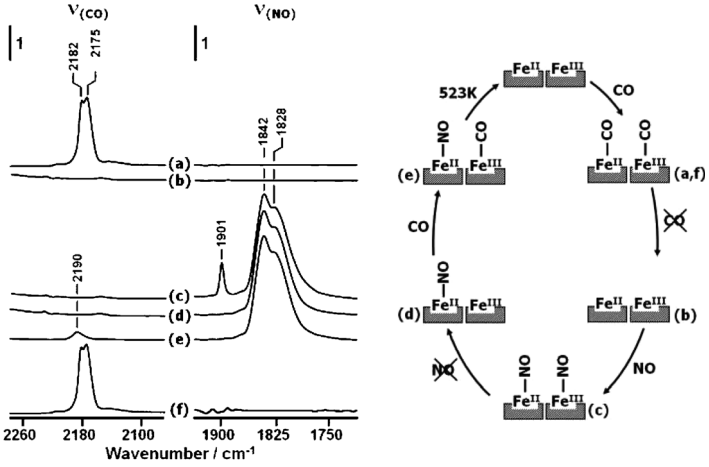

Figure 6. Left) IR spectra of MIL-100(Fe) (activated at 523 K for 12 h under He flow) under CO flow (10% in He) at RT (a), followed by a He flow (b), under NO flow (1% in He) (c), then flushed under He flow (d), followed by a CO flow (10% in He) (e) and finally, after reactivating the sample (523 K for 12 h under He flow) sending a CO flow (10% in He) again at RT (f). Right) Schematic representation of the adsorption–desorption mechanism.

stream containing 10% of CO in He, exactly the same bands were observed as before (not shown). This means that CO does not change the surface properties of MIL-100(Fe). Contrarily to the carbonyl species on Fe^{II}, the nitrosyl species on Fe^{II} are completely stable at room temperature under a He flow (Figures 6c and d). The band for Fe^{III} at $\tilde{\nu}=1901\ cm^{-1}$ completely disappears under a He flow, whereas the bands between $\tilde{\nu}=1800$–$1850\ cm^{-1}$ do not change. This behaviour could be used to selectively probe the sites on MIL-100(Fe). In fact, by sending a CO flow after NO and then helium treatment, only the carbonyl species for the Fe^{III} sites are observed because the Fe^{II} sites are blocked by NO (Figure 6e). The resulting spectrum displays the corresponding ν(CO) component at $\tilde{\nu}=2190\ cm^{-1}$ as well as the remaining ν(NO) modes in the $\tilde{\nu}=1800$–$1850\ cm^{-1}$ range. The intensity of the ν(NO) bands remains unchanged, showing that CO does not interact with NO adsorbed on the Fe^{II} sites. This may be considered as a peculiarity of the MOF structure, where the sites are practically isolated. After reactivating the sample and sending CO again, the same amount of species is observed (Figure 6f) as at the beginning (Figure 6a), which means that CO and even NO did not change the sample.

In summary, it was observed that neither CO nor NO changes the surface properties of MIL-100(Fe). Moreover, it is possible to block selectively all Fe^{II} CUSs by using NO. All these results allow us drawing a schematic view of the adsorption–desorption mechanism as represented in Figure 6 (right). Last but not least, we will now use this knowledge to explain the behaviour of MIL-100(Fe) for the separation of the propane/propene mixture.

Poisoning of the Fe^{II} CUSs and consequences for the separation effect: As we demonstrated above, it is possible to use NO to selectively block the Fe^{II} CUSs. Therefore, it is possible to poison one of the two possible sites (Fe^{II} and Fe^{III}) and to investigate the preferential gas sorption afterwards. This, until now, is one of the rare examples[3] where such selective site poisoning was possible, and the consequences for investigating material properties in action can be of paramount importance.

Figure 7 displays the adsorption of propene at RT with and without NO on the activated MIL-100(Fe) (He flow for 12 h at 523 K). The adsorption of propene dramatically decreases after blocking the Fe^{II} sites with NO as it is clearly shown by mass spectrometry (Figure 7A) and IR spectroscopy in the region of bands for adsorbed propene (Figure 7B). Moreover, Figure 7C indicates that the Fe^{II} sites poisoning by NO is still effective at the end of the C_3H_6/C_3H_8 adsorption experiment. MIL-100(Fe) activated at 523 K for 12 h can reach a separation factor over 100 under the conditions used here (low partial pressure of C3); however, after blocking the Fe^{II} sites with NO, this factor decreases to 5. All results of propane/propene adsorption with and without NO on the sample are summarized in Figures 8A and B. Both the amount of Fe^{II} sites and the separation effect increase with increasing the temperature (Figures 4 and 8A). After poisoning these sites, the separation effect decreases significantly (Figure 8B). This decrease is more emphasised with the increasing amount of Fe^{II} CUSs, which prove that propene has a strong affinity to Fe^{II} sites and that these sites are mainly responsible for the separation effect. However, we must also accentuate that the Fe^{III} CUSs also have a separation effect (Figure 8B) on the propane/propene mixture with a separation factor of around 4.

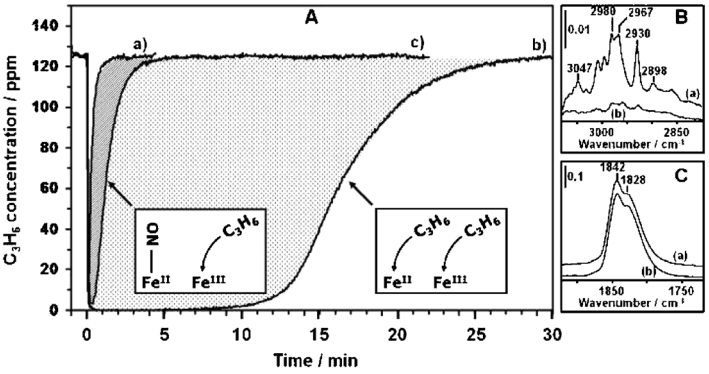

Figure 7. A) C_3H_6 adsorption on MIL-100(Fe) at RT followed by mass spectrometry ($m/z=41$) during C_3H_6/C_3H_8 separation experiments. a) Blank experiment without sample, b) experiment with sample activated at 523 K for 12 h, c) experiment with sample activated at 523 K for 12 h followed by NO adsorption at RT to block the Fe^{II} sites. B) IR spectra at saturation for C_3H_6/C_3H_8 adsorption on MIL-100(Fe) a) activated at 523 K for 12 h and b) activated at 523 K for 12 h followed by NO adsorption at RT. C) IR spectra of MIL-100(Fe) (activated at 523 K for 12 h) under a NO flow (1% in He) at RT and then flushed under a He flow (a) and after the C_3H_6/C_3H_8 adsorption experiment (b).

The fact that the separation factor sharply decreases by blocking Fe^{II} sites is due to the gas adsorption on Fe^{III} sites only, having a much lower affinity to propene. In the breakthrough test of propane/propene, a separation factor of 5.3 was found at a mixture pressure of 20 kPa.[27] This separation factor is a combination of the contribution of the Fe^{II} and Fe^{III} CUSs and is in good agreement with our observations. The Fe^{III} sites at higher partial pressure of the propane/propene mixture[27] are dominant due to their higher concentration in comparisons with Fe^{II} CUSs.[29]

Moreover, by considering a molar absorption coefficient of $\nu(CO)=4.8\ cm\,\mu mol^{-1}$ for the ν(CO) bands on Fe^{II} CUSs determined by in situ IR spectroscopy,[27] a quantitative analysis is possible and it results in a remarkable correlation between the mass spectrometric results of adsorbed propene and the concentration of adsorption sites (Figure 8C). Due to the limited detection of the Fe^{III} CUSs a quantitative analysis is more complicated for these sites, but it was still possible to plot the amount of propene adsorbed on Fe^{III} (followed by mass spectrometry) with the ν(NO) on the Fe^{III} band area (Figure 8D), finding again a good correlation. Therefore, both figures verify the results reported above.

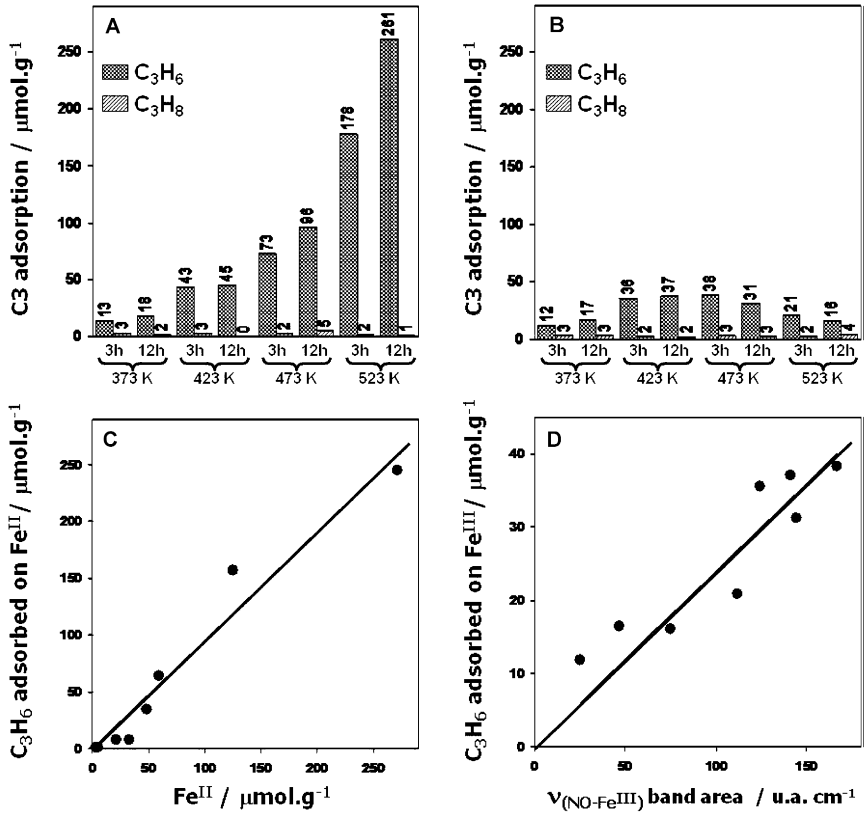

Figure 8. Propane/propene (C_3H_8/C_3H_6) adsorption on MIL-100(Fe) activated at different temperatures for 3 and 12 h followed by propane/propene adsorption A) before and B) after sending a NO flow through the sample. A comparison between the amount of adsorbed propene detected my mass spectrometry ($m/z=41$) and the amount determined with CO for C) Fe^{II} and D) Fe^{III}.

Conclusion

Mechanistic insight into the fundamentals of an operating material can only be acquired by using advanced characterisation methods that investigate the sample under operating conditions. This study is the first applying operando methodology in the field of MOFs. The reducible MIL-100(Fe) metal–organic framework was investigated for the separation of a propane/propene mixture. Breakthrough curves were obtained as in traditional separation column experiments, but having here the online monitoring of the material surface, which provides evidences on the adsorption sites. The qualitative and quantitative analyses of Fe^{II} and, to some extent, Fe^{III} sites were possible, upon different activation protocols. Details on the reduction mechanism of the iron site were obtained as well. Moreover, we were able to identify the nature of the active sites in the separation process by selective poisoning of one family of sites during the separation process, which constitutes a powerful and reliable method to describe reaction mechanisms. The hydrocarbon mixture flow after site poisoning was the gaining strategy to demonstrate the role of the Fe^{II}/Fe^{III} sites: it was clearly evidenced that the unsaturated Fe^{II} sites are mainly responsible for the separation effect of the propane/propene mixture, thanks to their affinity for the unsaturated C=C bonds. However, also for Fe^{III} sites a lower separation effect could be observed, which is important when a high operation pressure is used, due to the predominant concentration of Fe^{III} sites. This knowledge of the structure–activity relationship gives precious indications to optimise the sample. In other words, an iron MOF with a larger number of Fe^{II} CUSs is required in order to increase the separation effect for an alkane/unsaturated hydrocarbon mixture at low partial pressure. Moreover, such a material would also be interesting for NO trapping due to the high affinity of Fe^{II} sites for NO.

Experimental Section

Sample preparation and characterisation: MIL-100(Fe) was prepared from a hydrothermal reaction of trimesic acid with metallic iron, HF, nitric acid and H_2O. The composition of the reaction mixture was $1.0\,Fe^0$:0.67 1,3,5-BTC:2.0 HF:0.6 HNO_3:277 H_2O (1,3,5-BTC = 1,3,5-benzenetricarboxylic acid or trimesic acid). The reactant mixture was loaded into a Teflon autoclave heated up to the reaction temperature and kept at 423 K for 12 h. The pH remains acidic throughout the synthesis. The light orange solid product was recovered by filtration and washed with deionised water. The as-synthesised MIL-100(Fe) was purified further through a two-step processes by using hot water and ethanol. The purification has been performed by using boiling water at 353 K for 5 h in order to decrease the amount of residual unreacted ions (typically, 1 g of MIL-100(Fe) in 350 mL of water). Then, ethanol was boiled at 333 K for 3 h until there was no detection of coloured impurities in the mother liquor solution, thus resulting in the highly purified MIL-100(Fe). Finally, the solid was dried overnight at less than 373 K under a nitrogen atmosphere.

Structure of MIL-100(Fe): MIL-100(Fe) is a trivalent metal carboxylate MOF with the chemical composition $Fe_3O(H_2O)_2F_{0.81}(OH)_{0.19}\cdot(C_6H_5(CO_2)_3)_2\cdot n\,H_2O$ ($n\approx14.5$). As illustrated in Figure 9, MIL-100(Fe) consists

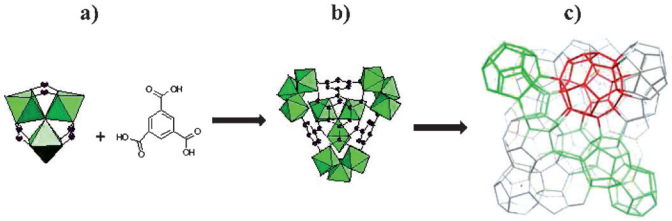

Figure 9. Structure of MIL-100. a) The secondary building unit (trimer of chromium, octahedral) and the organic liker (1,3,5-BTC). b) The hybrid supertetrahedron. c) Unit cell of MIL-100 with a schematic view of the MTN topology (MTN = zeolite socony mobil-thirty-nine) .

of iron trimers (the secondary building unit) and 1,3,5-benzene tricarboxylic (the organic linker), which construct the so-called supertetrahedra.[31] The resulting structure exhibits several interesting features: a mesoporous zeotype architecture (Figure 9c) with a MTN topology,[42] a huge cell volume ($V = 388000$ Å^3), two mesoporous cages (cage diameters: 25 and 29 Å—highlighted in Figure 9c as green (25 Å) and red (29 Å) cages—that are accessible through microporous windows (5 and 9 Å), a high BET surface area (>2000 m^2 g^{-1}) and a temperature stability under high vacuum until 523 K.[31] Moreover, it was already demonstrated for MIL-100(Cr) and MIL-100(Fe) by using in situ IR spectroscopy, that each metal octahedron possesses one terminal group, where H_2O, OH^- or F^- is adsorbed after the synthesis and it can transform in an under-coordinated site after temperature activation.[29,32] In the case of MIL-100(Fe), there is the possibility of the generation of iron CUSs with mixed valence Fe^{II}/Fe^{III} by temperature treatment.[27] This remarkable feature of MIL-100(Fe) requires a careful investigation of the reducibility of the framework. Despite the creation of Fe^{II} and Fe^{III} CUSs, the overall structure of MIL-100(Fe) does not change.[27]

IR operando experiments

IR operando system: The IR operando system, which was used for this study, is shown in Figure 10. This system is composed of four main parts: the infrared spectrometer, the IR reactor-cell, the gas flow set-up and the exhaust gas analysers. The cell was connected to the operando gas-system

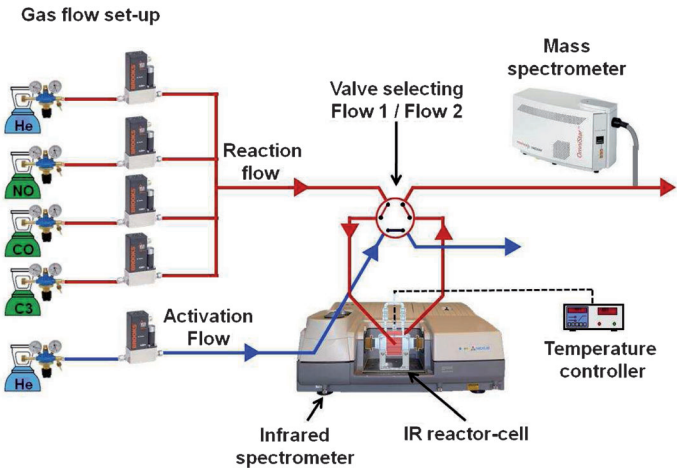

Figure 10. General view of the IR operando system.

including mass flow controllers for the introduction of gases into the lines. The two gas mixtures can be prepared and sent independently to the reactor-cell. The system allows investigating the exhaust gases (reactive and/or reaction products) by a quadrupole mass spectrometer (Pfeiffer Omnistar GSD 301). IR spectra (64 scans per spectrum) are collected with a Thermo Scientific Nicolet 6700 spectrometer, equipped with a MCT detector. More details can be found in references [43] and [44].

The "Sandwich" IR reactor-cell: The "sandwich" reactor-cell used in this study is an evolution of the operando cell developed by Saussey et al.,[43] which has proven its reliability over many years of operando studies.[45] The design of both the air cooling and the air tightness systems have been improved with the aim of widening its performance from the point of view of the domain of temperature (298–873 K). Figure 11 shows 3D views of this "sandwich" cell. The shape of the main part is a cylinder made of stainless steel that carries a spherical sample holder in its centre. That is where the sample is placed in the form of a self-supported wafer of 8–9 mg cm^{-2}. The heating system allows a maximum temperature of 873 K for the sample, whereas the air cooling system keeps the two ends of the cell below 573 K. The required tightness of the cell can be obtained by using Kalrez O-rings between the terminal KBr windows and the extremities of the cell. The rest of the space is filled by KBr windows, which limit the dead volume to 0.12 cm^3. The experiment was carried out

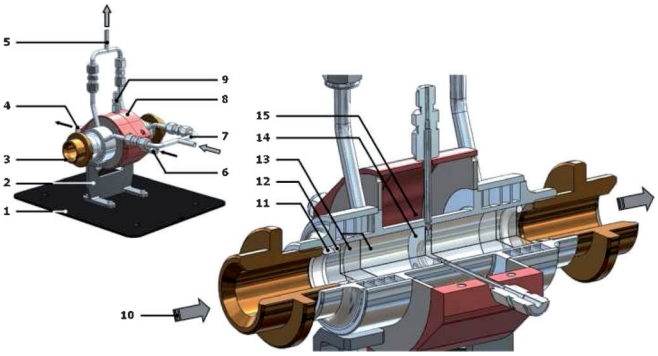

Figure 11. General and detailed views of the "sandwich" reactor-cell. 1 = Spectrometer base-plate, 2 = IR cell support, 3 = adjusting nut for air tightness, 4 = gas outlet, 5 = air cooling outlet, 6 = gas inlet, 7 = air cooling inlet, 8 = external shell, 9 = thermocouple location, 10 = IR beam, 11 = stainless steel ring, 12 = Kalrez O-ring, 13 = KBr windows, 14 = wafer holder, 15 = oven location.

at atmospheric pressure; gases are introduced onto the sample by a 1/8" OD pipe and collected on the opposite side of the sample holder.

Gas composition and experiment description: The gas compositions are the following: activation flow, He—total flow = 25 cm^{3}min^{-1} and reaction flow, propane (C_3H_8) 125 ppm and propene (C_3H_6) 125 ppm diluted in He—total flow = 25 cm^{3}min^{-1}. The consecutive steps for each experiment (a new pellet was used for each experiment) are: 1) The pre-treatment; samples have been previously heated under an activation flow (ramp 1,5 K min^{-1}) at 373, 423, 473 or 523 K for 3 or 12 h. 2) The temperature of the sample was decreased to 298 K. 3) Characterisation of MIL-100(Fe) CUSs was done by adding 10 % CO to the flow—CO is removed completely at the end of this step (switching to the activation flow). 4) The C_3H_8/C_3H_6 separation study was performed by switching to the reaction flow. After the concentration of C_3H_8/C_3H_6 returned to the original level of 125 ppm, the system was switched to the reaction flow for 30 min. 5) Followed by the addition of 1 % of NO to the reaction flow. After the concentration of NO returned to the original level the system was switched to the reaction flow for 30 min. 6) Finally, a C_3H_8/C_3H_6 flow of 125 ppm was sent again through the sample.

Acknowledgements

This work has been partially funded by MACADEMIA (www.macademia-project.eu), a 4-year Large-scale Integrating Collaborative Project funded by the European Community's Seventh Framework Programme (FP7/2007–2013) under grant agreement n° 228862 (Nanosciences, Nanotechnologies, Materials and New Production Technologies Theme), and by KRICT as "the Institutional Collaboration Program (KRICT, KK-1201-F0). S.W. acknowledges the Alexander von Humboldt foundation for a fellowship. Y.K.S., Y.K.H. and J.S.C. deeply acknowledge the international collaboration program KICOS, Korea for its financial support. The technical help of SOMINEX (Bayeux, Fr) for the Sandwich cell development is gratefully acknowledged as well.

[1] M. A. Banares, *Catal. Today* **2005**, *100*, 71.
[2] B. M. Weckhuysen, *Chem. Commun.* **2002**, 97.
[3] A. Vimont, F. Thibault-Starzyk, M. Daturi, *Chem. Soc. Rev.* **2010**, *39*, 4928.
[4] R. Schlögl, S. B. A. Hamid, *Angew. Chem.* **2004**, *116*, 1656; *Angew. Chem. Int. Ed.* **2004**, *43*, 1628.
[5] Themed issue: In-situ characterisation of heterogeneous catalysts *Chem. Soc. Rev.* **2010**, *39*, 4541.
[6] G. Férey, *Chem. Soc. Rev.* **2008**, *37*, 191.

[7] H. K. Chae, D. Y. Siberio-Perez, J. Kim, Y. Go, M. Eddaoudi, A. J. Matzger, M. O'Keeffe, O. M. Yaghi, *Nature* **2004**, *427*, 523.
[8] G. Férey, C. Mellot-Draznieks, C. Serre, F. Millange, J. Dutour, S. Surble, I. Margiolaki, *Science* **2005**, *309*, 2040.
[9] K. Koh, A. G. Wong-Foy, A. J. Matzger, *Angew. Chem.* **2008**, *120*, 689; *Angew. Chem. Int. Ed.* **2008**, *47*, 677.
[10] T. Devic, P. Horcajada, C. Serre, F. Salles, G. Maurin, B. Moulin, D. Heurtaux, G. Clet, A. Vimont, J.-M. Grenèche, B. L. Ouay, F. Moreau, E. Magnier, Y. Filinchuk, J. Marrot, J.-C. Lavalley, M. Daturi, G. Férey, *J. Am. Chem. Soc.* **2010**, *132*, 1127.
[11] Z. Wang, S. M. Cohen, *Chem. Soc. Rev.* **2009**, *38*, 1315.
[12] Y. K. Hwang, D.-Y. Hong, J.-S. Chang, S. H. Jhung, Y.-K. Seo, J. Kim, A. Vimont, M. Daturi, C. Serre, G. Férey, *Angew. Chem.* **2008**, *120*, 4212; *Angew. Chem. Int. Ed.* **2008**, *47*, 4144.
[13] J. Y. Lee, O. K. Farha, J. Roberts, K. A. Scheidt, S. B. T. Nguyen, J. T. Hupp, *Chem. Soc. Rev.* **2009**, *38*, 1450.
[14] L. Ma, C. Abney, W. Lin, *Chem. Soc. Rev.* **2009**, *38*, 1248.
[15] D. Farrusseng, S. Aguado, C. Pinel, *Angew. Chem.* **2009**, *121*, 7638; *Angew. Chem. Int. Ed.* **2009**, *48*, 7502.
[16] A. Corma, H. Garcıa, F. X. Llabres i Xamena, *Chem. Rev.* **2010**, *110*, 4606.
[17] A. U. Czaja, N. Trukhan, U. Müller, *Chem. Soc. Rev.* **2009**, *38*, 1284.
[18] J.-R. Li, R. J. Kuppler, H.-C. Zhou, *Chem. Soc. Rev.* **2009**, *38*, 1477.
[19] T. Düren, Y.-S. Bae, R. Q. Snurr, *Chem. Soc. Rev.* **2009**, *38*, 1237.
[20] S. S. Han, J. L. Mendoza-Cortés, W. A. Goddard, *Chem. Soc. Rev.* **2009**, *38*, 1460.
[21] L. J. Murray, M. Dinca, J. R. Long, *Chem. Soc. Rev.* **2009**, *38*, 1294.
[22] A. C. McKinlay, R. E. Morris, P. Horcajada, G. Férey, R. Gref, P. Couvreur, C. Serre, *Angew. Chem.* **2010**, *122*, 6400; *Angew. Chem. Int. Ed.* **2010**, *49*, 6260–6266.
[23] P. Horcajada, T. Chalati, C. Serre, B. Gillet, C. Sebrie, T. Baati, J. F. Eubank, E. Heurtaux, P. Clayette, C. Kreuz, J.-S. Chang, Y. K. Hwang, V. Marsaud, P.-N. Bories, L. Cynober, S. Gil, G. Férey, P. Couvreur, R. Gref, *Nat. Mater.* **2010**, *9*, 172.
[24] P. Horcajada, C. Serre, G. Maurin, N. A. Ramsahye, F. Balas, M. Vallet-Regi, F. Taulelle, G. Férey, *J. Am. Chem. Soc.* **2008**, *130*, 6774.
[25] P. Horcajada, C. Serre, M. Vallet-Regi, M. Sebban, F. Taulelle, G. Férey, *Angew. Chem.* **2006**, *118*, 6120; *Angew. Chem. Int. Ed.* **2006**, *45*, 5974.
[26] M. Maes, L. Alaerts, F. Vermoortele, R. Ameloot, S. Couck, V. Finsy, J. F. M. Denayer, D. E. De Vos, *J. Am. Chem. Soc.* **2010**, *132*, 2284.
[27] J. W. Yoon, Y.-K. Seo, Y. K. Hwang, J.-S. Chang, H. Leclerc, S. Wuttke, P. Bazin, A. Vimont, M. Daturi, E. Bloch, P. L. Llewellyn, C. Serre, P. Horcajada, J.-M. Grenèche, A. E. Rodrigues, G. Férey, *Angew. Chem.* **2010**, *122*, 6085; *Angew. Chem. Int. Ed.* **2010**, *49*, 5949.
[28] G. Férey, F. Millange, M. Morcrette, C. Serre, M.-L. Doublet, J.-M. Grenèche, J.-M. Tarascon, *Angew. Chem.* **2007**, *119*, 3323; *Angew. Chem. Int. Ed.* **2007**, *46*, 3259.
[29] H. Leclerc, A. Vimont, J.-C. Lavalley, M. Daturi, A. D. Wiersum, P. L. Llwellyn, P. Horcajada, G. Férey, C. Serre, *Phys. Chem. Chem. Phys.* **2011**, *13*, 11748.
[30] W. A. Herrebout, B. J. van der Veken, *J. Am. Chem. Soc.* **1997**, *119*, 10446.
[31] P. Horcajada, S. Surblé, C. Serre, D.-Y. Hong, Y.-K. Seo, J.-S. Chang, J.-M. Grenèche, I. Margiolaki, G. Férey, *Chem. Commun.* **2007**, 2820.
[32] A. Vimont, J.-M. Goupil, J.-C. Lavalley, M. Daturi, S. Surblé, C. Serre, F. Millange, G. Férey, N. Audebrand, *J. Am. Chem. Soc.* **2006**, *128*, 3218.
[33] A. Vimont, H. Leclerc, F. Maugé, M. Daturi, J.-C. Lavalley, S. Surblé, C. Serre, G. Férey, *J. Phys. Chem. C* **2007**, *111*, 383.
[34] K. I. Hadjiivanov, G. N. Vayssilov, *Adv. Catal.* **2002**, *47*, 307.
[35] K. I. Hadjiivanov, *Catal. Rev. Sci. Eng.* **2000**, *42*, 71.
[36] E. Ivanova, M. Mihaylov, K. I. Hadjiivanov, V. Blasin-Aubé, O. Marie, A. Plesniar, M. Daturi, *Appl. Catal. B* **2010**, *93*, 325.
[37] G. Magnacca, G. Cerrato, C. Morterra, M. Signoretto, F. Somma, F. Pinna, *Chem. Mater.* **2003**, *15*, 675.
[38] G. Berlier, G. Spoto, S. Bordiga, G. Ricchiardi, P. Fisicaro, A. Zecchina, I. Rossetti, E. Selli, L. Forni, E. Giamello, C. Lamberti, *J. Catal.* **2002**, *208*, 64.
[39] G. L. Miessler, D. A. Tarr in *Inorganic Chemistry*, Pearson Prentice Hall, Upper Saddle River, **2004**.
[40] G. Spoto, A. Zecchina, G. Berlier, S. Bordiga, M. G. Clerici, L. Basini, *J. Mol. Catal. A* **2000**, *158*, 107.
[41] M.-T. Nechita, G. Berlier, G. Ricchiardi, S. Bordiga, A. Zecchina, *Catal. Lett.* **2005**, *103*, 33.
[42] M. M. J. Treacy, J. B. Higgins in *Collection of Simulated XRD Powder Patterns for Zeolites*, 4th ed., Elsevier, Amsterdam, **2001**, and http://www.iza-structure.org/databases/.
[43] T. Lesage, C. Verrier, P. Bazin, J. Saussey, M. Daturi, *Phys. Chem. Chem. Phys.* **2003**, *5*, 4435.
[44] I. Malpartida, E. Ivanova, M. Mihaylov, K. Hadjiivanov, V. Blasin-Aubé, O. Marie, M. Daturi, *Catal. Today* **2010**, *149*, 295.
[45] a) T. Lesage, C. Verrier, P. Bazin, J. Saussey, S. Malo, C. Hedouin, G. Blanchard, M. Daturi, *Top. Catal.* **2004**, *30/31*, 31; b) F. Romero Sarria, O. Marie, P. Bazin, J. Saussey, J. Lesage, A. Guesdon, M. Daturi, *Catal. Today* **2006**, *113*, 87; c) T. Montanari, O. Marie, M. Daturi, G. Busca, *Appl. Catal. B* **2007**, *71*, 216; d) B. I. Mosqueda-Jiménez, A. Lahougue, P. Bazin, V. Harlé, G. Blanchard, A. Sassi, M. Daturi, *Catal. Today* **2007**, *119*, 73; e) T. Lesage, J. Saussey, S. Malo, M. Hervieu, C. Hedouin, G. Blanchard, M. Daturi, *Appl. Catal. B* **2007**, *72*, 166; f) P. Bazin, O. Marie, M. Daturi, *General Features of in situ and OPERANDO Spectroscopic Investigation in the Particular Case of deNOx Reactions in Past and Present in DeNOx Catalysis : From Molecular Modelling to Chemical Engineering* (Eds.: P. Granger, V. I. Parvulescu), Elsevier, Amsterdam, **2007**, Chapter 4, pp. 97–143; g) M. Ahrens, O. Marie, P. Bazin, M. Daturi, *J. Catal.* **2010**, *271*, 1; h) I. Malpartida, O. Marie, P. Bazin, M. Daturi, X. Jeandel, *Appl. Catal. B* **2011**, *102*, 190.

Received: March 24, 2012
Published online: August 13, 2012

